RSC Advances

ROYAL SOCIETY OF CHEMISTRY

www.rsc.org/advances

Journal Name

ARTICLE

Cleavage of Carbon Suboxide to Give Ketenylidene and Carbyne Ligands at a Reactive Tungsten Site: A Theoretical Mechanistic Study

Received 00th January 20xx,
Accepted 00th January 20xx

DOI: 10.1039/x0xx00000x

www.rsc.org/

Liang Pu,[a] Zhong Zhang,*[a,b] Qian-shu Li,[b] R. Bruce King*[c]

Reaction of $(MePPh_2)_4WCl_2$ with C_3O_2 has been shown experimentally to result in stepwise cleavage of the two C=C double bonds in C_3O_2 to give successively tungsten complexes containing phosphinoketenylidene and phosphinocarbyne ligands. The mechanism of such processes has been elucidated by density functional theory methods for the L_4WCl_2 (L = PMe_3, $PMePh_2$) systems. The triplet L_4WCl_2 reagents are found to proceed to singlet intermediates and products in a reaction sequence involving dissociation of a phosphine ligand, a triplet→singlet intersystem crossing, an initial C=C bond cleavage and a free phosphine attachment transition state. The first step is the rate-determining step with a *Gibbs* free energy barrier of 19.8 kcal/mol, and the formation of the stable phosphinoketenylidene intermediate is thermodynamically favorable. Further reaction of the phosphinoketenylidene intermediate to give the final phosphinocarbyne product is unusual because it is thermodynamically disfavored but kinetically feasible. The key steps involve loss of another phosphine ligand to give the transition state involving the cleavage of the second C=C bond of C_3O_2.

Introduction

Carbon suboxide, C_3O_2, was initially reported in 1906 as the product from double dehydration of malonic acid.[1] Despite the tendency of C_3O_2 to polymerize under relatively mild conditions,[2] its reactivity as the heterocumulene O=C=C=C=O, have led to its use as a reagent in organic chemistry as well as a ligand in transition metal chemistry. However, many interesting questions remain about its chemistry. Of particular interest is the use carbon suboxide as a synthetic source of "C_2O" and "C" fragments. In this connection, C_3O_2 has been used as a precursor for the production of graphene and carbon nanotubes by thermal decomposition and polymerization at relatively low temperatures.[3] Thus a temperature of only 180 °C is sufficient to produce carbon allotropes from C_3O_2 whereas nanotube synthesis otherwise requires much higher temperatures with an iron catalyst. The catalyst was found to play a key role in nanotube growth since without the catalyst the products instead were lamellar carbon nanoparticles.

In transition metal chemistry C_3O_2 functions as an activated olefin ligand, binding initially to the metal through a C=C double bond. The heavier congener C_3S_2 is also an olefin ligand, but it can bind to transition metals through either a C=C or a C=S double bond.[4,5] Subsequent reaction of the initially formed metal C_3O_2 complexes leads to ketenylidene complexes via oxidative addition. Thus in the reactions of C_3O_2 with platinum(0),[6] rhodium(I),[7] and nickel(0)[8] complexes, cleavage of a C=C double bond occurs to give products with a CO ligand and a C=C=O ketenylidene group. For the rhodium(I) complexes,[7] the ketenylidene group is liberated to undergo polymerization into $(C_2O)_n$ polymers. In addition, the M–H bonds in tungsten and rhenium hydrides add to a C=C double bond in C_3O_2 to form complexes containing a ketenyl group linked to a carbonyl group through a C–C single bond.[9] Theoretical calculations have explored the chemical bonding in C_3O_2 and its role as a π-acceptor in transition metal chemistry.[10]

Recent theoretical work by Esterhuysen and Frenking[11] have suggested an alternative view of C_3O_2 as $C(CO)_2$, i.e., a "carbon dicarbonyl" or "carbone." Since each of the CO groups in $C(CO)_2$ furnishes a lone pair to the central carbon atom, all four original valence electrons of the central carbon atom are available as two lone pairs. Such lone pairs can function as Lewis bases [e.g., bonding to an AuCl electrophile in $ClAu(C_3O_2)$] and/or participate in π→π* back bonding to the π* antibonding orbitals of the two outer CO groups. Such

[a] *College of Science, Northwest A&F University, Yangling, Shanxi 712100, P. R. China. Email: zhangzhong6@126.com; Fax:+86-29-87092226; Tel: +86-29-87092226*
[b] *School of Chemistry and Environment, South China Normal University, Key Laboratory of Theoretical Chemistry of Environment, Ministry of Education, Guangzhou, China 510006.*
[c] *Department of Chemistry and Center for Computational Quantum Chemistry, University of Georgia, Athens, Georgia 30602, USA. Email: rbking@uga.edu; Fax:+706-542-9454; Tel:+1-706-542-1901*

Electronic Supplementary Information (ESI) available: Fig. S1: Reaction paths of C_3O_2 binding to $WCl_2(PMe_3)_4$; Fig. S2: Reaction paths from int3 to P with an extrusion of one CO or Cl^- ligand; Table S1 Gibbs free energies of intermediates and TS from 1 to int3; Table S2 Gibbs free energies of intermediates and TS from int3 to P; Table S3: Natural charges of the atoms in C_3O_2 molecule and its fragments; Fig. S3: Geometries of P-ph with full $PMePh_2$ ligands with some labeled atoms; Table S4: Bond lengths and angles for $WCl_2(PMePh_2)_2(\eta^2_{CC}\text{-}C_2OPMePh_2)$; Tables S5-S28: Theoretical Cartesian coordinates for all complexes in the gas phase. See DOI:10.1039/x0xx00000x

bonding of C_3O_2 to a metal atom uses only the central carbon atom of the C_3O_2 ligand. The view of C_3O_2 as $C(CO)_2$ is related to the recently reported[12] stable boron dicarbonyl ArylB$(CO)_2$ [Aryl = 2,6-di(2,4,6-triisopropylphenyl)phenyl].

Another important reaction of C_3O_2 is the cleavage of its C=C double bonds leading ultimately to the formation of carbene, carbyne, or even carbide complexes. For example, C_3O_2 as well as some other heterocumulenes react with $WCl_2(PMePh_2)_4$ with subsequent cleavage of the C=C double bond initially coordinated to tungsten.[13-15] For C_3O_2, two CO molecules are sequentially lost consistent with its "carbon dicarbonyl" formation by Esterhuysen and Frenking.[11] In this way C_3O_2 can provide a synthon for free carbon atoms[13,14] not unlike the use of simple binary transition metal as reagents for metal deposition. The first loss of CO from C_3O_2 in this tungsten system gives the ketenylidene ligand C=C=O, which is trapped by coordination both with the central tungsten atom and coordination of a phosphine to the ketenylidene ligand. Further loss of the remaining CO group from the ketenylidene ligand occurs above 35 °C to give a carbide ligand which is stabilized by coordination with liberated phosphine to give a carbyne ligand of the type [W]≡C←PR_3.

The metal–carbon double and triple bonds in carbene and carbyne complexes are so reactive that they are used both catalytically and stoichiometrically for many organic reactions.[16,17] For example, metal–vinylidenes ($M=C=CR_2$) or allenylidenes ($M=C=C=CR_2$), as well as carbynes are known to be common catalytic intermediates and can initialize polymerization.[18] Thus metal vinylidenes are important species in many organic syntheses including alkyne polymerization and cycloaromatization.[19-21] Metal carbynes can function as polymerization catalysts for acetylenes and cycloalkenes.[22] These considerations suggest that the formation of carbene or carbyne species from C_3O_2 might relate to the growth of graphene and carbon nanotube materials. For this reason, a detailed understanding of the mechanism of stepwise C=C double bond cleavage in C_3O_2 is critically important for generating the carbene and carbyne metal complexes involved in catalytic processes. Unfortunately, the mechanism of this process has not been well understood. For this reason we undertook a density functional theory study of the C=C binding of C_3O_2 to $WCl_2(PMePh_2)_4$ and subsequent transformations to phosphine-stabilized ketenylidene and carbyne complexes.

Theoretical Methods

Density functional theory (DFT) methods have evolved as a practical and effective computational tool, especially for organometallic compounds.[23-29] In particular, the functional M06-L is found to be excellent for predicting geometries and vibrational frequencies. Furthermore, the M06-L method generally provides reliable results on the thermochemistry and thermochemical kinetics of main-group elements, transition metals, inorganic compounds, and organometallics.[30,31] Therefore we chose the M06-L functional for this study.

The basis set used for this work was a mixed double-ζ plus polarization (DZP) + Lanl2DZ basis set. Thus DZP is a double-zeta basis set, adding one set of d-functions on the heavy atoms and one set of p-functions on the hydrogen atoms. This DZP basis set for hydrogen, carbon, oxygen, sulfur, selenium, phosphorus and chloride was obtained by adding one set of pure spherical harmonic p(H)/d functions with orbital exponents $\alpha_p(H) = 0.75$, $\alpha_d(C) = 0.75$, $\alpha_d(O) = 0.85$, $\alpha_d(S) = 0.70$, $\alpha_d(Se) = 0.338$, $\alpha_d(P) = 0.60$ and $\alpha_d(Cl) = 0.60$, to the standard contracted DZ sets.[32-36] For tungsten, the effective core potential (ECP) basis sets Lanl2DZ was used.[37,38]

Geometry optimizations of all structures were performed at the DFT(M06-L)/DZP+Lanl2DZ level. Vibrational frequency calculations followed the optimizations to determine the thermodynamic properties. The transition state (TS) structures were located using TS and modredundant scan methods. Then the potential energy surface was obtained using the *Gibbs* free energy unless otherwise specified. Since the reported experimental work was carried out in toluene and chloroform, calculations in these solvents were also performed using the Polarizable Continuum Model (PCM)[39]. All calculations were carried out with the Gaussian 09 program.[40]

The experimental work[13,14] used methyldiphenyl-phosphine, $PMePh_2$, as the ligand. Since using $PMePh_2$ for all calculations was too computationally expensive, we chose a simpler phosphine, namely trimethylphosphine PMe_3, to locate the geometries of all of the structures and transition states in the reaction pathways. Subsequently the key structures were reconfirmed using $PMePh_2$ corresponding to the reported experimental work.

Upon checking the potential energy surfaces, we found one intersystem crossing between triplet and singlet spin states. Harvey's program[41] was used to locate the structures of the minimum energy intersystem crossing points (MECP).

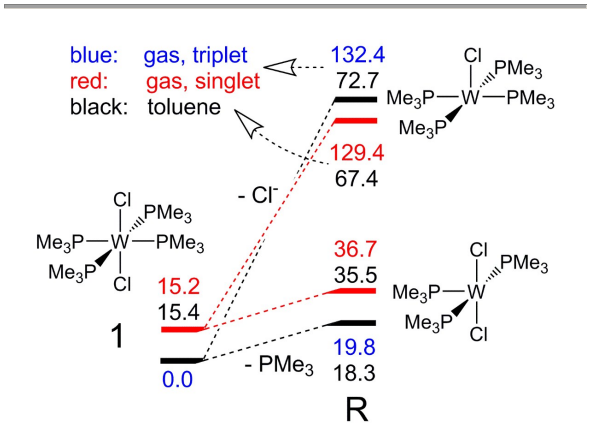

Fig. 1 Loss of PMe_3 or Cl^- from the triplet and singlet spin states of $WCl_2(PMe_3)_4$. The red and black paths refer to the singlet and triplet, respectively. The colored and black values represent the relative *Gibbs* free energies (kcal/mol), compared to singlet 1, in the gas phase and in toluene solution.

Results and Discussion

Generation of the reactive tungsten complex $WCl_2(PMe_3)_3$

These tungsten complexes appear to favor 16-electron structures owing to the steric effect of the phosphine groups and thus can exist in either triplet or singlet spin states. For the initial reactant *trans*-$W^{II}Cl_2(PMe_3)_4$ (**1**)[42,43], the triplet spin state is the lower energy spin state, lying 15.2 kcal/mol below the singlet spin state structure (Fig. 1). The octahedral coordination of the tungsten atom in $WCl_2(PMe_3)_4$ is too crowded to accept other incoming ligands leading to a seven-coordinate tungsten atom. Therefore, one or more ligands (chloride or PMe_3) must be removed from $WCl_2(PMe_3)_4$ before C_3O_2 can enter the tungsten coordination sphere. Chloride elimination from the triplet $WCl_2(PMe_3)_4$ requires a very high *Gibbs* free energy of 132.4 kcal/mol (gas phase) or 67.4 kcal/mol (toluene), whereas PMe_3 elimination requires only 19.8 kcal/mol (gas phase) or 18.3 kcal/mol (toluene), thus indicating the relative lability of the PMe_3 ligands. The 14-electron complex $WCl_2(PMe_3)_3$, obtained by losing a PMe_3 ligand from **1**, is also a triplet structure, lying 16.9 kcal/mol in *Gibbs* free energy below the corresponding singlet structure (Fig. 1). The resulting vacant site in $WCl_2(PMe_3)_3$ can now bind a C_3O_2 ligand. For our reported neutral species, most of the relative *Gibbs* free energy differences between the gas phase and solvent are found to be less than 2.0 kcal/mol, as expected. Thus, solvent effects are minor for neutral species. Therefore, only gas-phase results are discussed in this paper.

Mechanism of phosphinoketenylidene complex formation

Fully understanding the mechanism of stepwise cleavage of the C≡C bonds in C_3O_2 is critically important for preparing metal complexes containg the W≡C–PPh_3 ligand as well as related triply bonded W≡C–L analogues. Hillhouse and coworkers suggested a possible mechanism but not in detail.[13,14] We examined some possible pathways, both in the singlet and triplet spin states. We then selected the most favorable one shown in Fig. 2 as well as others given in Figs. S1 and S2 in the Electronic Supplementary Information.

As stated above, the first step is an extrusion of one PMe_3 ligand from triplet $WCl_2(PMe_3)_4$ (**1**) to give the intermediate $WCl_2(PMe_3)_3$ (**R**). However, loss of a second PMe_3 ligand from $WCl_2(PMe_3)_3$ seems unlikely since the dissociation *Gibbs* free energy is found to be relatively high at 33.0 kcal/mol (see Fig. S1 in the Electronic Supplementary Information). The intermediate **R** (Fig. 2) is therefore more likely to bind C_3O_2, suggested by the binding free energy of –18.0 kcal/mol for triplet **int1** or –30.9 kcal/mol for singlet **int1**. The triplet-singlet splitting is found to be 16.9 kcal/mol for **R**, but decreases to only 4.1 kcal/mol when C_3O_2 is added to **R** to give **int1**. This indicates that C_3O_2 in **R** is a strong field ligand like CO, thereby making the singlet reaction pathway more accessible.

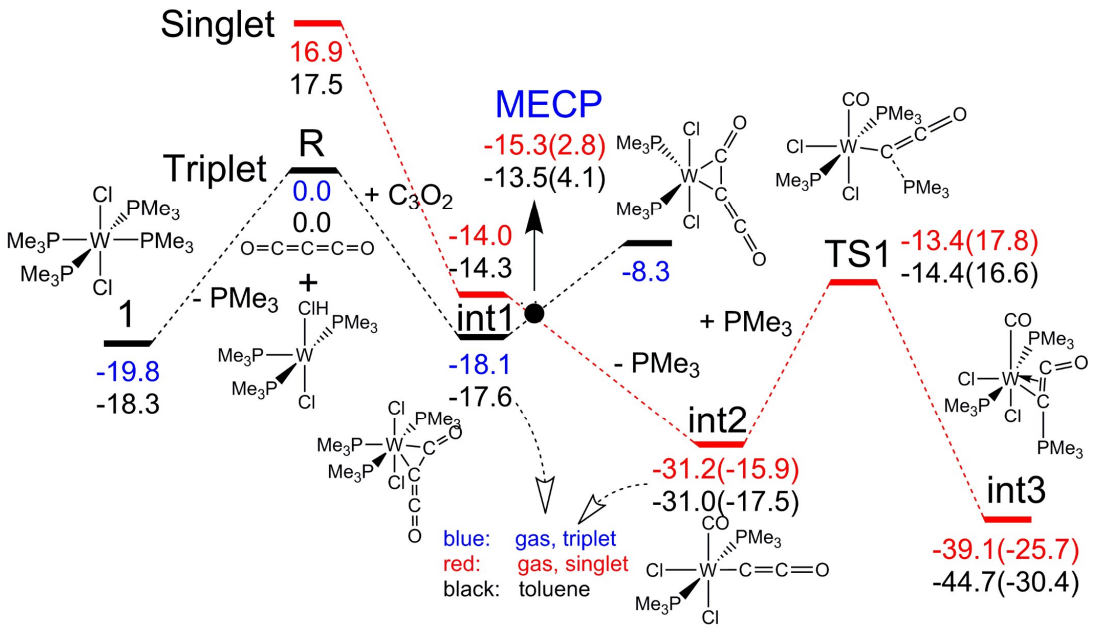

Fig. 2 A possible path from the reagents to the phosphinoketenylidene intermediate **int3** including two electron spin states, the singlet (red) and triplet (black), crossing at a MECP. The relative *Gibbs* free energies, all compared to **R** plus C_3O_2, and the *Gibbs* free energy changes from the previous step (in parentheses) are given in kcal/mol. The colored and black values represent the *Gibbs* free energies (kcal/mol) in gas phase and in toluene solution, respectively.

The experimental work[13,14] led to the isolation and characterization of the two important complexes **int3** and **P** in Figs. 2 and 4, respectively, which have been optimized in both singlet and triplet spin states. In both cases the singlet **int3** and **P** structures were found to have lower energies than the corresponding triplet structures, as indicated by an average singlet-triplet splitting of 15.9±1.6 kcal/mol (see Fig. S1 in the Electronic Supplementary Information). Therefore, from the initial triplet **R** to the final singlet **P** via the singlet **int3**, a MECP must be present in both channels. In this connection, all of the stationary points as well as transition states were examined in two different spin states (Fig. 2). The $WCl_2(PMe_3)_2(CO)(C_2O)$ intermediate (**int2**), derived from **int1** by simultaneous cleavage of the C1=C0 bond (Fig. 3) and loss of a PMe_3 ligand, is predicted to be a singlet because of its lower energy of 18.2 kcal/mol relative to the corresponding triplet. It is thus reasonable to suspect that the structure of MECP is more similar to that of **int1** (small splitting) rather than to that of **int2** (large splitting).

Harvey's program[41] was then used to locate the MECP structure (Fig. 3). The obvious change in structure of the MECP compared with **int1** is the decrease in the C1-C0-W-Cl dihedral angle from 52.0° for **int1** to 3.5° for the MECP. This means that in **int1** the C_3O_2 ligand is not in the same plane as the two chlorine atoms whereas in the MECP the C_3O_2 ligand and the two chlorine atoms become nearly planar. The W-C0 and W-C1 distances are found to decrease from 2.128 Å and 2.089 Å (triplet) to 2.061 Å and 2.037 Å (singlet), respectively, suggesting strengthening of the W-C bonds in going from **int1** to MECP. Meanwhile, the increased C0-C1 distance of 1.484 Å in MECP from 1.427 Å in **int1** suggests stronger activation (oxidation) of C_3O_2 in MECP relative to **int1**. This can be verified from the lower total natural charge of –0.281 on the C_3O_2 fragment in the MECP and larger charge of –0.309 in **Int1** (Table S3 in the Electronic Supplementary Information). Moreover, the natural charges on C0 and C1 change from –0.516 and 0.561 in **int1** to –0.491 and 0.557 in MECP, respectively. The *trans* W-PMe_3 bond in MECP is weakened owing to the *trans*-effect of C_3O_2 since the *trans*-W-P distance is elongated from 2.614 Å in **int1** to 2.653 Å in MECP. Accordingly, the MECP structure is disfavored with respect to loss of the PMe_3 group *trans* to C_3O_2. At this point the energy of the triplet pathway increases and that of the singlet pathway decreases so that the two pathways cross. For the triplet pathway, $WCl_2(PMe_3)_3(\eta^2_{CC}\text{-}C_3O_2)$ first becomes another intermediate $WCl_2(PMe_3)_2(\eta^2_{CC}\text{-}C_3O_2)$ by losing a PMe_3 ligand and then goes through a transition state to become $WCl_2(CO)(PMe_3)_2(C_2O)$ (see Fig. S1 in the Electronic Supplementary Information). For the singlet pathway loss of the second PMe_3 ligand leads to simultaneous cleavage of the C=C bond of C_3O_2 thereby giving the ketene complex **int2**.

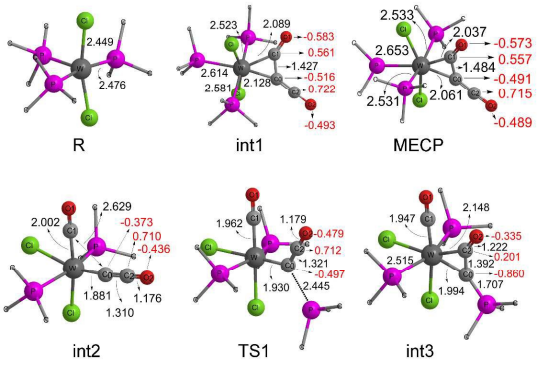

Fig. 3 Structures along the possible reaction pathway in Fig. 2 with some bonding data in black and natural charges in red (arrows from the atoms). The methyl hydrogen atoms are omitted for clarity.

The intermediate **int2** can be regarded as a singlet C=C=O carbene stabilized by coordination to tungsten. The very stable intermediate (**int3**) is formed by using free PMe_3 rather than the coordinated PMe_3 to attack the carbene carbon atom C0, simultaneously converting the monohapto η^1-C_2O ligand into a dihapto η^2-C_2O ligand stabilized by coordination of PMe_3. This process needs to cross a transition state (**TS1**) with an activation free energy of 17.8 kcal/mol, then **TS1** releases 25.7 kcal/mol. Thus the W=C=C=O unit is unstable in **int2**, which was not isolated in the experimental work. The natural charge on the carbene atom (C0) atom in the C_2O fragment becomes more negative from –0.373 in **int2**, to –0.497 in **TS1** and –0.860 in **int3**. The charge on the C_2O fragment also becomes more negative in this reaction sequence, i.e., –0.099 in **int2**, –0.264 in **TS1** and in –0.994 **int3**. These observations indicate the enhancement of the M→C_2O back donation to the C_2O fragment in the sequence **int2** < **TS1** < **int3** thereby strengthening the bonding between the metal center and the C_2O fragment. However, the bonding mode of the C_2O fragment changes in the sequence **int2** → **TS1** → **int3**. Thus in **int2** the C0 atom is sp hybridized with a linear W=C=C=O bond, while in **int3** the C0 atom has bent sp^2 hybridization after coordination with PMe_3. This bonding change is reflected by the W-C0 bond distance that changes from 1.881 Å in **int2** to 1.930 Å in **TS1** and 1.994 Å in **int3** (Fig. 3). It is very difficult to break a chemical bond with sp hybridized atoms, whereas chemical bonds with sp^2 hybridized atoms are more readily broken. Accordingly, the C0-C2 bond distance lengthens from 1.310 Å to 1.321 Å and 1.392 Å in the sequence **int2** → **TS1** → **int3**, indicating that the second C0=C2 double bond of C_3O_2 is also activated in **int3**. However the C0-C2 bond (1.392 Å) in **int3** is still viable so that **int3** is a stable intermediate and can be isolated experimentally.

Conversion of the triplet reagent $WCl_2(PMe_3)_4$ to the singlet intermediate **int3** occurs through an intersystem crossing. This process is thermodynamically favorable since the *Gibbs* free energy of **int3** is 19.3 kcal/mol below that of $WCl_2(PMe_3)_4$. For the entire pathway in Fig. 2, the rate-limiting step is then the first step, namely the loss of the first PMe_3 ligand from $WCl_2(PMe_3)_4$, requiring a *Gibbs* free energy of 19.8 kcal/mol. The transition state **TS1** is the second important step, whereas the intersystem crossing is a minor energetic

factor. Conversely, the reverse reaction has a higher energy barrier of 25.7 kcal/mol from **int3** to **TS1**. Thus the reverse reaction is unlikely to proceed under ambient conditions owing to thermodynamically and kinetically unfavorable factors.

Mechanism of phosphinocarbyne formation

The phosphinocarbyne complex, **P**, is obtained from **int3** by CO elimination.[13,14] However, it appears to be thermodynamically disfavored since **P** has a higher free energy of 17.6 kcal/mol than **int3** (Fig. 4). In fact, the most common method of preparing a ketenylidene complex such as **int3** is the carbonylation of a carbyne ligand such as that in **P**.[13,14] However, experimental work[14] shows that **P** can be obtained from **int3** by mild heating to 35°C for 48 hr. in chloroform solution. Conversely, treatment of **P** with carbon monoxide at 20 °C does not give **int3**. These observations suggest that the reaction direction is kinetically rather than thermodynamically controlled. We therefore searched for a reaction pathway with a suitably high activation free energy for the conversion of **P** to **int3**.

The tungsten atom in **int3** is six-coordinate by being bonded to the phosphinoketenylidene ligand, one carbonyl group, two chlorides, and two trimethylphosphine ligands and has a 16-electron configuration similar to $WCl_2(PMe_3)_4$. Cleavage of the C=C bond of the ketenylidene ligand converts **int3** into a complex with an 18-electron configuration but with an unfavorable tungsten coordination number of seven. We also scan the energy surface, with every step optimized, by slowly elongating the ketenylidene C=C bond. However we cannot locate a stable intermediate with seven ligands. Thus the first possible step in the pathway for conversion of **int3** into **P** should be loss of one ligand. Therefore, the dissociation *Gibbs* free energies of CO, Cl^-, and PMe_3 ligands from **int3** were compared and the corresponding energy data and possible reaction paths, in the singlet and triplet spin states and in the gas phase and in chloroform solution, are supplied in Fig. 4 and Fig. S2 and Table S2 in the Electronic Supplementary Information. The results show that dissociation of either CO or Cl^- from **int3** in the gas phase is very difficult requiring a free energy greater than 40 kcal/mol (41.2 and 123.8 kcal/mol for CO and Cl^-, respectively, see Fig. S2 in the Electronic Supplementary Information). Even in chloroform, extrusion of Cl^- still requires 61.2 kcal/mol (see Fig. S2 in the Electronic Supplementary Information). However, the dissociation free energy of PMe_3 is only 18.0 kcal/mol (gas) or 16.3 kcal/mol (chloroform). This implies that the ligand dissociated from **int3** in the first step of its conversion to **P** should be PMe_3. This information is used to derive the reaction pathway shown in Fig. 4. The corresponding intermediates are shown in Fig. 5.

The first step in the conversion of **int3** to **P** thus involves a loss of one PMe_3 ligand to give **int4**, requiring a free energy of 18.0 kcal/mol. The loss of PMe_3 is accompanied by migration of the chlorine atom *trans* to CO in **int3** to *trans* to the remaining PMe_3 ligand owing to the large *trans* effect of CO and the steric effect of the phosphinoketenylidene ligand. Therefore the tungsten coordination in **int4** is approximately square pyramidal with a vacancy *trans* to the CO group. However, the electron density on the tungsten atom is reduced in going from **int3** to **int4** owing to loss of a strong σ-donor PMe_3 ligand. This reduces the M→L back donation

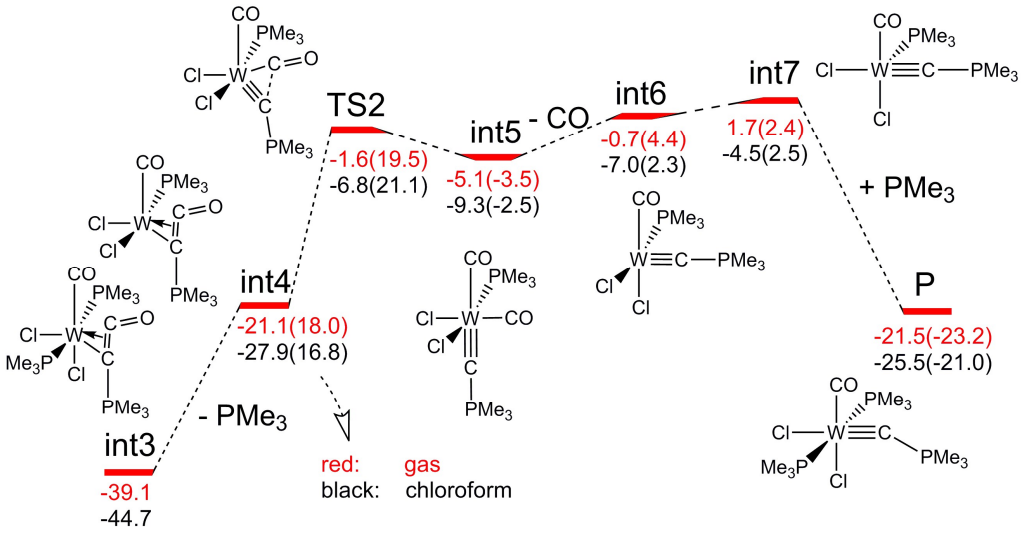

Fig. 4 Possible reaction pathway from the phosphinoketenylidene intermediate to the phosphinocarbyne product, all in singlet states. The red and black values represent the relative *Gibbs* free energies (kcal/mol), compared to **R** plus C_3O_2 (Fig. 2), in the gas phase and in chloroform, respectively.

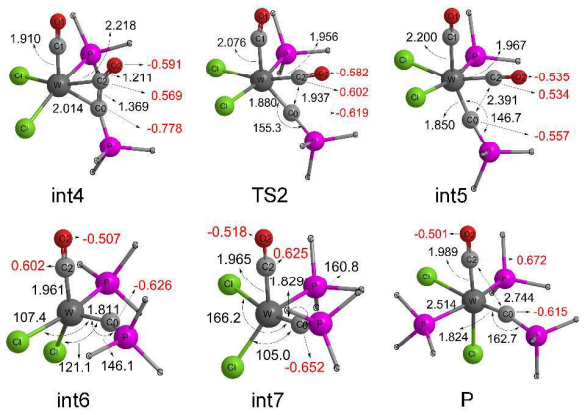

Fig. 5 Structures along the possible reaction pathway in Fig. 2 with some bonding data in black and natural charges in red (arrows from the atoms). The methyl hydrogen atoms are omitted for clarity.

thereby slightly lengthening the W-C0 and W-C2 bonds from 1.994 Å and 2.148 Å (Fig. 3) to 2.014 Å and 2.218 Å (Fig. 5), respectively. In addition the C0-C2 bond is shortened from 1.392 Å (Fig. 3) to 1.369 Å (Fig. 5).

The phosphinoketenylidene C=C double bond in **int4** then undergoes cleavage to give the phosphinocarbyne intermediate, **int5**, through a transition state, **TS2**. The activation free energy of this transition state is 19.5 kcal/mol, which is slightly larger than the PMe_3 dissociation free energy of **int3**. The structure of **TS2** is so close to that of **int5** that the **TS2**→**int5** conversion reduces the free energy by only 3.5 kcal/mol. This is mainly because the major structural change from **TS2** to **int5** is the substantial lengthening of the C0-C2 distance from 1.937 Å to 2.391 Å (Fig. 5). However, the C0-C2 distance in **TS2** is already so much longer than a normal carbon-carbon bond that its further lengthening has little effect on the energy. In contrast, the very large stretching of the C0-C2 bond from 1.369 Å to 1.937 Å in going from **int4** to **TS2** changes a C=C double bond to a C¨¨C non-bonding interaction. This is expected to lead to a substantial change in energy. Both **TS2** and **int5** contain the phosphinocarbyne ligand with short W≡C triple bond distances of 1.880 and 1.850 Å, respectively, as compared with a W-C0 distance of 2.014 Å in **int4**. However, the phosphinocarbyne ligand has a large *trans*-influence, lengthening the *trans* W-CO distance from 1.910 Å in **int4** to 2.200 Å in **int5**. This *trans*-influence reduces the *Gibbs* free energy for dissociation of the CO ligand *trans* to the carbyne to only 4.4 kcal/mol. The resulting facile dissociation of this CO group gives another intermediate **int6**. Note that **int6** and its successors as depicted in Fig. 5 are rotated approximately 90° counterclockwise on the paper plane compared with its predecessors.

This intermediate **int6** is a relatively high-energy coordinatively unsaturated intermediate containing a five-coordinate tungsten atom (Fig. 5). The loss of the strongly back-bonding CO group in going from **int5** to **int6** strengthens the back donation of the tungsten atom to the remaining ligands leading to slight shortening of the bonds from the tungsten atom to both the phosphinocarbyne ligand and the remaining CO group. Addition of one of the liberated PMe_3 ligands from an earlier step to **int6** is all that is needed to give the final product **P**. However, such addition is expected to be unfavorable since the vacant coordination site is *trans* to the phosphinocarbyne, which has a large *trans* effect. On the other hand, one vibrational mode in **int6** around 70 cm^{-1} includes a swing of the W–Cl bond, located *trans* to the only remaining PMe_3 ligand in the tungsten coordination sphere, between the *cis* and *trans* position of the phosphinocarbyne ligand. Thus the *Gibbs* free energy required for this chlorine to migrate *trans* to W≡C-PMe_3 is only 2.4 kcal/mol. This migration produces an intermediate **int7**, having the vacant coordination site *trans* to the PMe_3 ligand with a nearly linear Cl-W-C0 angle of 166.2°. Attaching a free PMe_3 ligand to the vacant coordination site in **int7** to give the product, **P**, is now energetically favorable, releasing 23.2 kcal/mol.

The final product $WCl_2(CO)(PMe_3)_2(\equiv CPMe_3)$ (**P**) is a stable octahedral hexacoordinate structure. The PMe_3 unit in the phosphinocarbyne ligand is essentially a phosphonium ion with a formal positive charge. Therefore, a neutral phosphino-carbyne ligand is formally a four-electron donor to the tungsten atoms with three electrons coming from the W≡C triple bond and the fourth electron indirectly from the phosphorus atom. The tungsten atom in **P** thus has the favored 18-electron configuration. In **P** the W≡C triple bond shortens to 1.824 Å and the W-C0-P angle to the phosphinocarbyne ligand is slightly bent at 162.7°.

In going from **int3** to **P**, there seems to exist an obviously much larger free energy barrier, namely 55.5 kcal/mol, from **int3** to **TS2**. However, between **int3** and **TS2,** there lies an intermediate **int4** that splits the large free energy barrier into two smaller ones and leads to a more feasible reaction (Fig. 4). Thus the rate-determining step in going from **int3** to **P** is that from **int4** to the transition state **TS2** (Fig. 4), requiring a *Gibbs* free energy of approximately 20 kcal/mol, rather than the step from **int3** to **TS2**. This *Gibbs* free energy barrier suggests that the reaction could proceed under ambient conditions. However, the experiments show that **int3** is so stable at ambient temperature that it can be isolated in the crystalline state. The reaction with $PMePh_2$ as the phosphine actually requires slight heating at 35 °C for 48 hr.[13,14] This is because the forward process is totally endothermic (17.6 kcal/mol). Therefore an energy compensation is needed from heating. In addition, vaporization of CO from chloroform is a key driving force for conversion of **int3** to **P**. The overall *Gibbs* free energy of 17.6 kcal/mol leads to a very small equilibrium constant ($K^{\ominus}$) in chloroform solvent. The concentration of CO in the solvent is readily decreased by warming, thus driving the reaction equilibrium in the forward direction. Therefore, at ambient temperature **int3** is stable enough to be isolated in the crystalline state for determination of its structure by X-ray crystallography. Additionally, we suspect that the forward reaction rate at ambient temperature might be very slow so

that conversion of **int3** to **P** needs 48 hr although it is energetically preferred.

While looking back to the reverse reaction channel, i.e. from **P** to **int3**, this process can occur spontaneously since it is thermodynamically favored as releasing a *Gibbs* free energy of 17.6 kcal/mol, and is kinetically feasible owing to the dominant free energy barrier of 23.2 kcal/mol (Fig. 4). However, the experimental work[13,14] showed that carbonylation of the phosphinocarbyne complex **P** back to the ketenylidene complex **int3** does not occur at 20 °C and 1 atm CO. This discrepancy might arise from the following three factors. First, the larger activation *Gibbs* free energy barrier (23.2 kcal/mol) from **P** to **Int3** leads to an even lower reaction rate than for the forward process. As a result, a longer reaction time might be required to observe the carbonylation of the metal phosphinocarbyne intermediate **int3**. Second, carbonylation of phosphinocarbyne might be not a simple reaction, since the preparation of ketene ligands[44] from carbonylation of metal carbene requires high CO pressure for increasing the reaction rate as well as for making the equilibrium move to the backward. Finally, the W≡C triple bond in **P** is a high energy structural feature and therefore is suspected to be highly reactive towards carbonylation. However, Hillhouse and co-workers did not supply more details about the experimental conditions, even though Pandolfo's group[45] provided suggestions that this reaction was reversible. Recently, a bridged μ_2-CPh carbyne was reported to couple a CO to form spontaneously a PhC=C=O bridge.[46] However, losing a CO from the PhC=C=O bridge required heating (energy compensation). Therefore, a carbyne ligand is suspected to be more stable than a PhC=C=O or Ph_3PC=C=O ligand. We suggest that further experimental investigation is therefore necessary for preparing the novel Ph_3P=C=C=O ligand by carbonylation of a phosphinocarbyne ligand at a lower temperature, longer reaction time, and especially higher CO pressure.

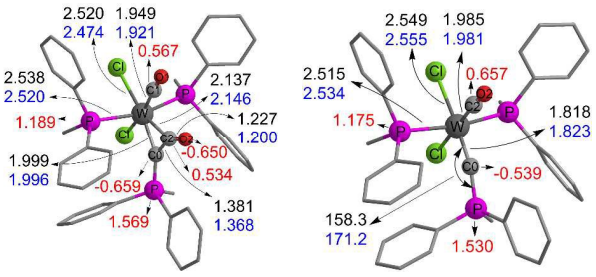

Int3-ph (0.0) **P-ph** (18.5)

Fig. 6 Geometries of **int3-ph** and **P-ph** with some bonding and natural charge data. The top (black) and the bottom (blue) numbers represent the present work and experiment,[14] respectively, and the red numbers show the natural charge. Note that the experimental data for **P-ph** are from the complex $WCl_2(CO)(PMePh_2)_2(\equiv CPPh_3)$.

Structures with PMePh2 ligands

The discussion above is based on the simplest phosphine that is a reasonable model for the experimental chemistry, namely trimethylphosphine, PMe_3. However, the experimental work used methyldiphenylphosphine, $PMePh_2$. In order to determine the significance of the choice of phosphine for these reactions, the structures of the species actually isolated and characterized structurally, namely **int3** and **P** with $PMePh_2$ ligands, labelled as **int3-ph** and **P-ph**, respectively, were optimized (Fig. 6 and Table S4 in the Electronic Supplementary Information) and the optimized geometries were compared with experimental data. However, note that the experimental data for **P** are taken from triphenylphosphinocarbyne complex $WCl_2(CO)(PMePh_2)_2(\equiv CPPh_3)$ since experimental data are not available for the methyldiphenylphosphinocarbyne complex $WCl_2(CO)(PMePh_2)_2(\equiv CPMePh_2)$. The key bonding data change very little when the phosphine is changed from PMe_3 in **int3** to $PMePh_2$ in **int3-ph**. Thus the critical W-C0, W-C1, C0-C2, and C2-O2 distances in **int3** (Fig. 3) and **int3-ph** (Fig. 6) are essentially unchanged within ±0.01 Å. The largest difference is the shortening of the W-C2 bond from 2.148 Å in **int3** to 2.137 Å in **int3-ph**. For **P-ph**, the critical bond distances are also very similar to those of **P**, with almost identical W-CO and W-P bond distances. The W-C0 distance and the W-C0-P angle of the carbyne ligand are slightly shorter and smaller, respectively, in **P-Ph** relative to **P**. These results show that the simplified PMe_3 ligand provides a reasonable model for our theoretical study.

The *Gibbs* free energy of the **P-ph** complex relative to **int3-ph** is 18.5 kcal/mol (Fig. 6), which is slightly larger than the 17.6 kcal/mol energy of **P** relative to **int3** (Fig. 4). For **int3-ph**, the differences between the calculated key bonding interatomic distances and the experimental distances from X-ray crystallography[14] agree within ±0.03 Å, suggesting that our DFT calculation is very reliable. In particular, the interatomic distances in the key fragment (1.999, 2.137, and 1.381 Å for W-C0, W-C2, and C0-C2, respectively), namely the phosphinoketenylidene ligand, agree within ±0.013 Å of the experimental values (1.996, 2.146, and 1.368 Å for W-C0, W-C2, and C0-C2, respectively) except for the C2-O2 distance. For **P-ph**, the calculated W-C0 distance of 1.818 Å is slightly shorter than the experimental value of 1.823 Å. However, our predicted W-C0-P angle for the phosphinocarbyne ligand in **P-ph** of 158.3° differs significantly from the experimental value of 171.2°. This discrepancy might arise from the fact that the phosphinocarbyne ligand in **P-ph** is W≡CPMePh$_2$ whereas that in the experimental complex is W≡CPPh$_3$. The greater steric demand of PPh_3 relative to $PMePh_2$ might account for this difference. The predicted interatomic distances for **P-ph** with a W≡CPMePh$_2$ ligand and the experimental interatomic distances for the corresponding complex with a W≡CPPh$_3$ ligand,[14] including the critical W-Cl, W-P and W-C2 bonds, agree within ±0.02 Å.

Conclusions

Carbon suboxide (C_3O_2) is known experimentally to react with $WCl_2(PMe_3)_4$ to form a stable phosphinoketenylidene intermediate and a phosphinocarbyne product by sequentially breaking its two C=C bonds. The mechanism of this process has been investigated using density functional theory. Carbon suboxide strongly prefers bonding to tungsten as well as other transition metals through its C=C bond rather than its C=O bond. The mechanism of this reaction of C_3O_2 with $WCl_2(PMe_3)_4$ involves intersystem crossing from a triplet reaction channel to a singlet reaction channel, with a low free energy barrier. The MECP structure is found to be close to the first reaction intermediate where the smallest singlet-triplet splitting energy is located. The first C=C cleavage then occurs, followed by migration of a free phosphine ligand to the resulting C_2O ligand to give a phosphine-stabilized stable ketenylidene intermediate. Cleavage of the second C=C bond from the original C_3O_2 follows loss of a phosphine ligand from this phosphineketenylidene intermediate with dissociation of one CO ligand. Addition of a phosphine ligand gives the final phosphinocarbyne product. The reaction pathway from the phosphinoketenylidene intermediate to the final phosphine-carbyne complex is unusual since it is thermodynamically disfavored. However, it can proceed because it is kinetically favorable during heating as shown by the calculated energy barriers.

Acknowledgements

We are indebted to the National Natural Science Foundation of China (Grant 21303138), the China Postdoctoral Science Foundation (Grants 2013M540660 and 2014T70817), the Chinese Universities Scientific Fund (Grant 2014YB028), the Fundamental Research Funds for the Central Universities (Grant 2452015425), the PhD Research Startup Foundation of Northwest A&F University (Grant 20100203185), and the U. S. National Science Foundation (Grant CHE-1057466) for support of this research.

Notes and references

1 O. Diels and B. Wolf, *Ber. Dtsch. Chem. Ges.*, 1906, **39**, 689.
2 J. S. auf der Günne, J. Beck, W. Hoffbauer and P. Krieger-Beck, *Chem. Eur. J.*, 2005, **11**, 4429–4440.
3 M. W. Shao, D. B. Wang, G. H. Yu, B. Hu, W. C. Yu and Y. T. Qian, *Carbon*, 2004, **42**, 183–185.
4 A. P. Ginsberg, W. E. Lindsell and W. E. Silverthorn, *Transactions New York Academy of Sciences*, 1971, **33**(3), 303–312.
5 A. P. Ginsberg and W. E. Silverthorn, *J. Chem. Soc. D.*, 1969, 823–824.
6 G. Paiaro and L. Pandolfo, *Angew. Chem. Int. Ed.*, 1981, **20**, 288–289.
7 G. Paiaro and L. Pandolfo, *Angew. Chem. Int. Ed.*, 1981, **20**, 289–290.
8 A. K. List, M. R. Smith III and G. L. Hillhouse, *Organometallics*, 1991, **10**, 361–362.
9 G. L. Hillhouse, *J. Am. Chem. Soc.*, 1985, **107**, 7772–7773.
10 M. Casarin, L. Pandolfo and A. Sassi, *Organometallics*, 2002, **21**, 2235–2239.
11 C. Esterhuysen and G. Frenking, *Chem. Eur. J.*, 2011, **17**, 9944–9956.
12 H. Braunschweig, R. D. Dewhurst, F. Hupp, M. Nutz, K. Radacki, C. W. Tate, A. Vargas and Q. Ye, *Nature*, 2015, **522**, 327–330.
13 A. K. List and G. L. Hillhouse, *J. Am. Chem. Soc.*, 1988, **110**, 4855–4856.
14 A. K. List and G. L. Hillhouse, *Organometallics*, 1989, **8**, 2010–2016.
15 J. C. Bryan, S. J. Geib, A. L. Rheingold and J. M. Mayer, *J. Am. Chem. Soc.*, 1987, **109**, 2826–2828.
16 M. I. Bruce, *Chem. Rev.*, 1998, **98**, 2797–2858.
17 C. Bruneau and P. H. Dixneuf, *Angew. Chem. Int. Ed.*, 2006, **45**, 2176–2203.
18 C. Bruneau and P. H. Dixneuf, *Metal Vinylidenes and Allenylidenes in Catalysis: From Reactivity to Applications in Synthesis*, Wiley-VCH, Weinheim, Germany, 2008.
19 C. Bruneau and P. H. Dixneuf, *Acc. Chem. Res.*, 1999, **32**, 311–323.
20 B. M. Trost, *Acc. Chem. Res.*, 2002, **35**, 695–705.
21 B. M. Trost, M. U. Frederiksen and M. T. Rudd, *Angew. Chem. Int. Ed.*, 2005, **44**, 6630–6666.
22 T. J. Katz, T. H. Ho, N. Y. Shih, Y. C. Ying and Van I. W. Stuart, *J. Am. Chem. Soc.*, 1984, **106**, 2659–2668.
23 M. Brynda, L. Gagliardi, P. O. Widmark, P. P. Power and B. O. Roos, *Angew. Chem. Int. Ed.*, 2006, **45**, 3804–3807.
24 N. Sieffert and M. Bühl, *J. Am. Chem. Soc.*, 2010, **132**, 8056-8070.
25 P. Schyman, W. Lai, H. Chen, Y. Wang and S. Shaik, *J. Am. Chem. Soc.*, 2011, **133**, 7977–7984.
26 R. D. Adams, W. C. Pearl, Y. O. Wong, Q. Zhang, M. B. Hall and J. R. Walensky, *J. Am. Chem. Soc.*, 2011, **133**, 12994–12997.
27 R. Lonsdale, J. Olah, A. J. Mulholland and J. N. Harvey, *J. Am. Chem. Soc.*, 2011, **133**, 15464–15474.
28 L. Crawford, D. J. Cole-Hamilton, E. Drent and M. Bühl, *Chem. Eur. J.*, 2014, **20**, 13923–13926.
29 H. Zhekova, M. Krykunov, J. Autschbach and T. Ziegler, *J. Chem. Theory Comput.*, 2014, **10**, 3299–3307.
30 Y. Zhao and D. G. Truhlar, *J. Chem. Phys.*, 2006, **125**, 194101.
31 B. S. Marendrapurapu, N. A. Richardson, A. V. Copan, M. L. Estep, Z. Yang and H. F. Schaefer, *J. Chem. Theory Comput.*, 2013, **9**, 2930–2938.
32 T. H. Dunning, *J. Chem. Phys.*, 1970, **53**, 2823–2834.
33 T. H. Dunning and P. J. Hay, *in Methods of Electronic Structure Theory*, ed. H. F. Schaefer, Plenum, New York, 1977, pp. 1–27.
34 S. Huzinaga, *J. Chem. Phys.*, 1965, **42**, 1293–1302.
35 A. J. H. Wachters, *J. Chem. Phys.*, 1970, **52**, 1033–1036.
36 D. M. Hood, R. M. Pitzer and H. F. Schaefer III, *J. Chem. Phys.*, 1979, **71**, 705–712.
37 W. R. Wadt and P. J. Hay, *J. Chem. Phys.*, 1985, **82**, 284–298.
38 P. J. Hay and W. R. Wadt, *J. Chem. Phys.*, 1985, **82**, 299–310.
39 J. Tomasi, B. Mennucci, and R. Cammi, *Chem. Rev.*, 2005, **105**, 2999-3093.
40 M. J. Frisch, *et al.*, *Gaussian 09, Revision B.01*, Gaussian, Inc., Wallingford CT, 2010.
41 J. N. Harvey, M. Aschi, H. Schwarz and W. Koch, *Theor. Chem. Accts.*, 1998, **99**, 95–99.
42 P. R. Sharp, *Organometallics*, 1984, **3**, 1217–1223.
43 S. F. Nelsen, R. W. Alder, R. B. Sessions, K. D. Asmus, K. O. Hiller and M. Göbl, *J. Am. Chem. Soc.*, 1980, **102**, 1430–1431.
44 G. L. Geoffroy and S. L. Bassner, *Adv. Organomet. Chem.*, 1988, **21**, 1.
45 R. Berani, M. Casarin and L. Pandolfo, *Coord. Chem. Rev.*, 2003, **236**, 15–33.
46 M. A. Alvarez, M. E. García, D. García-Aivó, M. E. Martínez, M. A. Ruiz, *Organometallics*, **2011**, *30*, 2189–2199.

Table of Contents Synopsis

Cleavage of Carbon Suboxide to Give Ketenylidene and Carbyne Ligands at a Reactive Tungsten Site: A Theoretical Mechanistic Study

Liang Pu,[a] Zhong Zhang,*[a,b] Qian-shu Li,[b] R. Bruce King*[c]

The reaction of $(MePPh_2)_4WCl_2$ with C_3O_2 has been reported to result in stepwise cleavage of the two C=C double bonds in C_3O_2 to give successively tungsten complexes containing phosphineketenylidene and phosphinecarbyne ligands. The mechanism of this reaction has been elucidated to process a minimum energy intersystem crossing point from triplet to singlet for $L_3WCl_2(C_3O_2)$ by using density functional theory.